Intelligent and Converged Networks
2024, 5(1): 19−27

ISSN 2708-6240
DOI: 10.23919/ICN.2024.0002

Cascaded channel decoupling based solution for RIS regulation matrix

Yajun Zhao*

Abstract: This article presents a pioneering solution to address the challenges of reconfigurable intelligent surface (RIS), employing a cascaded channel decoupling strategy. This novel method streamlines the RIS regulation matrix by dividing the process of electromagnetic wave modulation into two separate sub-processes: virtual receiving response and virtual regular transmission, resulting in the decoupling of the RIS cascaded channel. Furthermore, the paper explores the practical implementation of this channel decoupling method in two typical scenarios, including single-user and multi-user access, offering detailed insights into its application. Through numerical simulations, the article demonstrates the effectiveness and reduced complexity of the proposed scheme in enhancing the efficiency of the RIS regulation matrix.

Key words: reconfigurable intelligent surface; channel decoupling; receiving matrix; transmitting matrix

1 Introduction

The manipulation of electromagnetic waves has been a longstanding objective within the realm of research, constrained primarily by the inherent fixed electromagnetic characteristics of natural materials, restricting this capability to transmitters and receivers. The advent of reconfigurable intelligent surface (RIS) has engendered significant enthusiasm among both academic and industrial communities, driven by their profound potential to exert control over the wireless environment. Consequently, RIS technology has swiftly garnered momentum in both scholarly investigation and practical industrial implementations. It is increasingly recognized as a pivotal and promising technology in the evolution of 5G-Advanced and 6G networks[1, 2].

RIS is a two-dimensional programmable metamaterial consisting of a large number of electromagnetic elements arranged periodically. By changing the state of its switching elements (such as PIN diodes, varactor diodes, and liquid crystals), it can reconstruct the arrangement of an electromagnetic response structure on the surface of an element, thereby altering the electromagnetic response characteristics[3]. The introduction of RISs has transformed the naturally uncontrollable electromagnetic propagation environment into a human-controllable one, potentially bringing about a new channel paradigm. However, accurate dynamic electromagnetic wave regulation relies on the efficient and precise solution of the RIS regulation matrix. There are many literature discussions on the channel model of RIS[4, 5]. A significant body of literature offers different mechanisms for solving the RIS regulation matrix to enable channel regulation[6, 7], wireless energy transmission[8, 9], information modulation[10], and to address coexistence problems in RIS networks[11, 12]. However, the introduction of cascaded channels after the implementation of a RIS poses significant challenges to solving the RIS regulation matrix. In our previous article[13], we briefly described the basic idea of a channel decoupling mechanism to address this challenge. In this article, we conduct an in-depth discussion and performance evaluation based on further study.

This article makes contributions and innovations

• Yajun Zhao is with Beijing Institute of Technology, Beijing 100081, China and also with ZTE Corporation, Beijing 100029, China. E-mail: zhao.yajun1@zte.com.cn.
∗ To whom correspondence should be addressed.
Manuscript received: 2023-08-07; accepted: 2023-10-11

through the introduction of a novel cascaded channel decoupling model and algorithm for resolving the RIS regulation matrix. The proposed model delineates a fresh approach to the decoupling of RIS cascaded channels, segmenting the electromagnetic wave regulation process into two distinct sub-processes: virtual reception response and regulation transmission. This delineation leads to the partitioning of the RIS regulation matrix into two constituent components: the reception response matrix and the regulation transmission matrix. The cascaded channel decoupling model achieves the segmentation of the cascaded channel into two autonomous and separable channels. For each of segmented channels, the conventional direct path channel methodology can be employed to resolve the transmitter and receiver’s beamforming matrices, effectively accomplishing the decoupling of RIS cascaded channels and significantly reducing the complexity associated with solving the RIS regulation matrix. This innovative approach is denoted as the “**cascaded channel decoupling based solution**”. Building upon this newly introduced cascaded channel decoupling model, the article proceeds to examine scenarios involving single-user access and multi-user access, presenting corresponding solutions for both contexts.

The article is structured as follows. Section 2 presents the system model and analyzes the challenge of solving the RIS regulation matrix due to the introduction of cascaded channels. Section 3 introduces the cascaded channel decoupling schemes for solving the RIS regulation matrix. The proposed decoupling model is further discussed in two scenarios: single user equipment (UE) access and multi-UE access, with corresponding solutions provided. Section 4 presents the numerical results and discussion. Finally, in Section 5, a conclusion is drawn.

2 System model and challenge

2.1 System model

For the downlink of the RIS-assisted wireless communication system shown in Fig. 1, a node B (NB) is configured with M antennas, and a RIS is configured

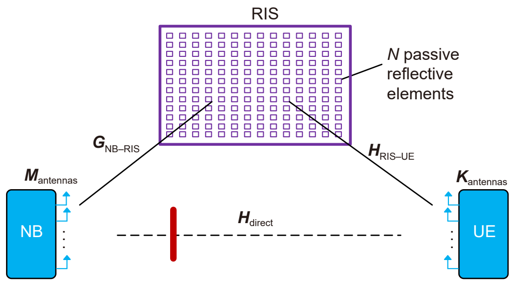

Fig. 1 System model.

with N elements that serve users with each having K antennas. Due to the introduction of the RIS into the system, the system model includes the traditional direct channel component $\boldsymbol{H}_{\rm direct} \in \boldsymbol{C}^{K\times M}$ between the NB and UE and the cascaded channel $\boldsymbol{H}_{\rm cascaded} \in \boldsymbol{C}^{K\times M}$ regulated by the RIS, where the cascaded channel $\boldsymbol{H}_{\rm cascaded} \in \boldsymbol{C}^{K\times M}$ consists of the segmented channel $\boldsymbol{G}_{\rm NB-RIS} \in \boldsymbol{C}^{N\times M}$ between the NB and RIS and the segmented channel $\boldsymbol{H}_{\rm RIS-UE} \in \boldsymbol{C}^{K\times N}$ between the RIS and UE.

The downlink channel $\boldsymbol{H}_{\rm DL}$ can be represented as Eq. (1).

$$H_{\rm DL} = \boldsymbol{H}_{\rm cascaded} + \boldsymbol{H}_{\rm direct} = \boldsymbol{H}_{\rm RIS-UE}^{\rm H}\boldsymbol{\Theta}\boldsymbol{G}_{\rm NB-RIS} + \boldsymbol{H}_{\rm direct} \tag{1}$$

where $\boldsymbol{\Theta} = {\rm diag}(\theta_1, \theta_2, \ldots, \theta_N)$ is the regulation matrix at the RIS with θ_n representing the regulation coefficient for the n-th RIS element.

Solving blind spots is a typical application of RIS. Generally, in this case, the signal of the direct channel between NB and UE is very weak. To simplify the discussion process, it is assumed that direct channels $\boldsymbol{H}_{\rm direct}$ can be ignored without losing generality. Then, Eq. (1) of the RIS channel model can be rewrite as Eq. (2).

$$\boldsymbol{H}_{\rm DL} = \boldsymbol{H}_{\rm cascaded} = \boldsymbol{H}_{\rm RIS-UE}^{\rm H}\boldsymbol{\Theta}\boldsymbol{G}_{\rm NB-RIS} \tag{2}$$

The received signal $\boldsymbol{Y}$ at the UE side can accordingly be represented as Eq. (3).

$$\boldsymbol{Y} = \boldsymbol{H}_{\rm RIS-UE}^{\rm H}\boldsymbol{\Theta}\boldsymbol{G}_{\rm NB-RIS}\boldsymbol{F}\boldsymbol{x} + \boldsymbol{W} \tag{3}$$

where $\boldsymbol{F}$ is the transmitting matrix at the NB side, $\boldsymbol{x} = [x_1, x_2, \ldots, x_L]^{\rm T}$ satisfying $E\{\boldsymbol{x}\boldsymbol{x}^{\rm H}\} = \boldsymbol{I}$ is the transmit signal vectors of the NB, and $\boldsymbol{W}$ is additive white Gaussian noise at the UE side. Without losing generality, in this article, we assume that the RIS regulation is lossless and has a unitary constraint on the regulation matrix, that is, the power of the incident wave is equal to that of the reflected wave $\boldsymbol{\Theta}\boldsymbol{\Theta}^{\mathrm{H}} = \boldsymbol{I}$.

2.2 Challenges of cascaded channels

Equation (2) illustrates the positioning of the RIS regulation coefficient matrix $\boldsymbol{\Theta}$ between two segmented channel matrices, specifically the channel $\boldsymbol{G}_{\mathrm{NB-RIS}}$ between the NB and RIS and the channel $\boldsymbol{H}_{\mathrm{RIS-UE}}$ between the RIS and UE. From a mathematical perspective, directly resolving the matrix components between two matrices within the context of matrices with general structures is an intricate task. Consequently, existing literature frequently resorts to iterative optimization or other search methods to address this challenge. In the works referenced in Refs. [14–18], a prevalent approach involves the joint iteration for optimizing both the base station's beamforming matrix and the RIS regulation matrix. This process encompasses the determination of optimization criteria and the base station's beamforming matrix, followed by the search and optimization of the RIS regulation matrix. Subsequently, the RIS regulation matrix is determined, and the beamforming matrix of the base station is searched and optimized. This iterative optimization process is iterated multiple times. Nonetheless, it is essential to acknowledge that these iterative optimization methodologies confront several formidable challenges, including elevated computational complexity, protracted processing cycles, and uncertain convergence rates.

In Ref. [19], the special case where a UE is equipped with a single antenna, i.e., $K = 1$, was discussed. According to the analysis of the literature, because the channel $\boldsymbol{H}_{\mathrm{RIS-UE}} \in \boldsymbol{C}^{1\times N}$ between the RIS and UE is a matrix structure of $1\times N$, in the cascaded channel model, after matrix transformation, the regulation matrix of the RIS can exchange positions with the $\boldsymbol{H}_{\mathrm{RIS-UE}}$ matrix for matrix multiplication. That is, Eq. (2) of the RIS channel model can be expressed as Eq. (4) by matrix transformation.

$$\boldsymbol{H}_{\mathrm{DL}} = \boldsymbol{H}^{\mathrm{H}}_{\mathrm{RIS-UE}}\boldsymbol{\Theta}\boldsymbol{G}_{\mathrm{NB-RIS}} = \boldsymbol{\Theta}\mathrm{diag}(\boldsymbol{H}^{\mathrm{H}}_{\mathrm{RIS-UE}})\boldsymbol{G}_{\mathrm{NB-RIS}} \tag{4}$$

The transformed channel model, as represented in Eq. (4), facilitates the derivation of the regulation matrix $\boldsymbol{\Theta}$ through the use of an analytical decomposition matrix $\mathrm{diag}(\boldsymbol{H}^{\mathrm{H}}_{\mathrm{RIS-UE}})\boldsymbol{G}_{\mathrm{NB-RIS}}$. However, this mathematical transformation ceases to be applicable when the UE is equipped with multiple antennas.

As of the present, there is a conspicuous absence of publicly available research addressing the effective resolution of the issue concerning UEs equipped with multiple antennas in a straightforward manner, despite the prevalent use of multi-antenna UEs in real-world scenarios. Consequently, it becomes imperative to seek a simplified and efficacious approach to tackle the regulation matrix $\boldsymbol{\Theta}$ in such instances.

3 Channel decoupling for solving RIS regulation matrix

The previous analysis shows the complex nature of popular iterative optimization solutions, making them not practical for real-world engineering applications. It becomes imperative to seek a straightforward methodology for resolving the RIS regulation matrix $\boldsymbol{\Theta}$, one that accommodates both single-antenna and multi-antenna scenarios.

3.1 Channel decoupling mechanism

Based on the previous analysis of Eq. (2) of the RIS cascaded channel model, it is evident that the RIS regulation matrix $\boldsymbol{\Theta}$ is coupled between the two sub-channel matrices, resulting in high complexity when solving the RIS regulation matrix. A natural idea is that if the cascaded channel can be decoupled and the two sub-channels of the cascaded channel can be decomposed separately, the complexity of the solution can be significantly reduced.

A fresh perspective on the RIS system model reveals that the regulation of incident electromagnetic waves by the RIS can be logically divided into two distinct virtual sub-processes: the receiving response sub-process and the output regulation sub-process. However, prevailing solution methodologies tend to treat RIS regulation as a unified process, necessitating the simultaneous resolution of the coupled segmented channels within the cascaded channels.

Upon closer examination of these two virtual sub-processes, it becomes evident that the receiving response virtual sub-process within the RIS can be conceptualized as a virtual receiver. The optimal design of this virtual receiver can be predicated upon established principles of traditional optimal receiver design, contingent upon the channels traversed by the incoming signal. Given the multi-antenna array nature of the RIS, optimizing this virtual receiver can be transformed into the optimization of the ideal receiving matrix. Subsequent to processing by the virtual response sub-process, the incoming signal undergoes channel equalization, ensuring the restoration of the original signal without distortion from channel effects before mapping to the outbound antennas. On the other hand, the output regulation sub-process within the RIS can be likened to a virtual transmitter featuring a virtual multi-antenna array. The optimal design of this virtual transmitter can be devised based on established principles of traditional optimal transmitter design, which, in turn, is reliant upon the channel characteristics between this virtual transmitter and its corresponding receiver. Given that this virtual transmitter is also a multi-antenna array, the optimal transmitter design transforms into the optimization of the transmit precoding matrix for the RIS antenna array.

Drawing upon the aforementioned analysis, it becomes evident that the optimal processing matrices governing the two virtual sub-processes within RIS regulation can be properly characterized as the receiving response matrix $\boldsymbol{\Theta}_1$ and the output regulation matrix $\boldsymbol{\Theta}_2$ of the RIS, respectively. The receiving response matrix $\boldsymbol{\Theta}_1$ corresponds to the sub-channel $\boldsymbol{G}_{\text{NB}-\text{RIS}}$ connecting the transmitter (NB) and the RIS, while the output regulation matrix $\boldsymbol{\Theta}_2$ pertains to the segmented channel $\boldsymbol{H}_{\text{RIS}-\text{UE}}^{\text{H}}$ established between the RIS and the receiver (UE). In other words, the receiving response matrix $\boldsymbol{\Theta}_1$ can be calculated based on the segmented channel $\boldsymbol{G}_{\text{NB}-\text{RIS}}$, and the output regulation matrix $\boldsymbol{\Theta}_2$ can be calculated based on the segmented channel $\boldsymbol{H}_{\text{RIS}-\text{UE}}^{\text{H}}$. This conceptual framework, thus, offers a means to decompose the comprehensive RIS regulation matrix $\boldsymbol{\Theta}$ into two constituent sub-matrix components: the receiving response sub-matrix $\boldsymbol{\Theta}_1$ and the output regulation sub-matrix $\boldsymbol{\Theta}_2$.

Taking the downlink (DL) channel as an example, the series equations for the sub-process of the cascaded channel correlation processing of RIS are as follows.

1. Expression for RIS receiving response virtual sub-process. The downlink signal $\boldsymbol{Y}_{\text{DL,RIS,IN}}$ incident on RIS through the channel between NB and RIS is denoted as Eq. (5) before being processed by RIS.

$$\boldsymbol{Y}_{\text{DL,RIS,in}} = \boldsymbol{G}_{\text{NB}-\text{RIS}}\boldsymbol{F}\boldsymbol{x} \tag{5}$$

The signal $\boldsymbol{X}_{\text{RIS}}$ expression (Eq. (6)) of the downlink signal $\boldsymbol{Y}_{\text{DL,RIS,in}}$ incident on the RIS panel is processed by the RIS virtual response sub-process (also known as the virtual receiving sub-process).

$$\boldsymbol{X}_{\text{RIS}} = \boldsymbol{\Theta}_1\boldsymbol{Y}_{\text{DL,RIS,in}} = \boldsymbol{\Theta}_1\boldsymbol{G}_{\text{NB}-\text{RIS}}\boldsymbol{F}\boldsymbol{x} \tag{6}$$

In Eqs. (5) and (6), $\boldsymbol{F}$ is the multi-antenna precoding matrix of NB side; $\boldsymbol{x} = [x_1, x_2, \cdots, x_L]^{\text{T}}$ is the data sequence sent by NB, satisfying $E\{\boldsymbol{x}\boldsymbol{x}^{\text{H}}\} = \boldsymbol{I}$. Since RIS is passive regulation, there is no additive white Gaussian noise term in Eq. (5).

2. Expression for RIS output modulation virtual sub-process. The signal $\boldsymbol{X}_{\text{RIS}}$ processed by the RIS virtual response sub-process is further processed by the RIS virtual regulation sub-process (also called the virtual transmission sub-process), and the processed output signal $\boldsymbol{X}_{\text{DL,RIS,out}}$ is expressed as Eq. (7).

$$\boldsymbol{X}_{\text{DL,RIS,out}} = \boldsymbol{\Theta}_2\boldsymbol{X}_{\text{RIS}} = \boldsymbol{\Theta}_2\boldsymbol{\Theta}_1\boldsymbol{G}_{\text{NB}-\text{RIS}}\boldsymbol{F}\boldsymbol{X} \tag{7}$$

The signal $\boldsymbol{X}_{\text{DL,RIS,out}}$ processed by the two virtual subprocesses of RIS flows to the UE channel through the RIS, so the downlink signal $\boldsymbol{Y}_{\text{DL,UE}}$ at the UE receiving end is expressed as Eq. (8).

$$\boldsymbol{Y}_{\text{DL,UE}} = \boldsymbol{H}_{\text{RIS}-\text{UE}}^{\text{H}}\boldsymbol{X}_{\text{DL,RIS,out}} + \boldsymbol{W} \tag{8}$$

where $\boldsymbol{H}_{\text{RIS}-\text{UE}}^{\text{H}}$ is the channel between RIS and UE; $\boldsymbol{W}$ is the additive Gaussian white noise matrix of UE.

3. To combine the above sub-processes, and get a complete equation. By combining Eqs. (5)–(8), Eq. (9) can be obtained. Equation (9) is the expression for the whole process of the downlink signal reaching the UE receiver after being processed by two virtual sub processes of RIS.

$$\boldsymbol{Y}_{\mathrm{DL,UE}} = \boldsymbol{H}_{\mathrm{RIS-UE}}^{\mathrm{H}} \boldsymbol{\Theta}_2 \boldsymbol{\Theta}_1 \boldsymbol{G}_{\mathrm{NB-RIS}} \boldsymbol{F}\boldsymbol{x} + \boldsymbol{W} \tag{9}$$

Comparing Eqs. (3) and (9), the expression (Eq. (10)) of RIS regulation matrix can be obtained naturally.

$$\boldsymbol{\Theta} = \boldsymbol{\Theta}_2 \boldsymbol{\Theta}_1 \tag{10}$$

Then Eq. (2) of the downlink cascaded channel model can be written as Eq. (11).

$$\boldsymbol{H}_{\mathrm{DL}} = \boldsymbol{H}_{\mathrm{RIS-UE}}^{\mathrm{H}} \boldsymbol{\Theta}_2 \boldsymbol{\Theta}_1 \boldsymbol{G}_{\mathrm{NB-RIS}} \tag{11}$$

The concept described above bears a resemblance to the analog beamforming matrix employed by the transmitter and the analog beamforming response matrix used by the receiver within the context of conventional large-scale MIMO hybrid beamforming[20]. However, in traditional large-scale MIMO scenarios, this form of processing typically entails the direct decomposition of the direct path channel between the transmitter (NB) and the receiver (UE). Conversely, within the cascaded channel model of RIS, the acquisition of the RIS regulation matrix $\boldsymbol{\Theta}$ cannot be accomplished through the direct decomposition of the channel matrix. This necessitates a fresh perspective where the regulatory actions of the RIS are conceptualized as the two aforementioned virtual sub-processes.

Remark 1 The regulation mechanism of the RIS undergoes a conceptual division into two virtualized sub-processes: the receiving response sub-process (or virtual receiving sub-process) governing incident electromagnetic waves and the output regulation sub-process (or virtual transmitting sub-process) controlling emitted electromagnetic waves. These two virtual sub-processes align with the two distinct segmented channels within the cascaded channel model. Consequently, the independent decomposition of the two segmented channel matrices leads to the derivation of two virtual processing sub-matrices. This approach effectively accomplishes the decoupling of the RIS cascaded channels, resulting in a noteworthy reduction in the computational complexity associated with resolving the RIS regulation matrix.

Remark 2 It is imperative to underscore that Eq. (5) must adhere to a minimum of two crucial conditions. Firstly, the two segmented channels, denoted as $\boldsymbol{H}_{\mathrm{RIS-UE}}$ and $\boldsymbol{G}_{\mathrm{NB-RIS}}$, should be amenable to decomposition into a receiving response matrix and a transmitting regulation matrix, respectively. Secondly, in light of the passive regulatory nature of the RIS, the regulation matrix is typically expected to adhere to constant modulus constraints.

Next, we will further explore specific solution examples of $\boldsymbol{\Theta}_1$ and $\boldsymbol{\Theta}_2$ for single-user access scenarios and multi-user access scenarios, respectively.

3.2 Channel decoupling for single-user access

The expressions encompassed by Eqs. (5)–(11) are readily applicable in the context of single-user access scenarios. In this section, we will commence by exploring the implementation of the proposed scheme within a single-user access scenario.

For the sake of clarity and to maintain generality, we employ singular value decomposition (SVD) as an analytical tool to elucidate the solution procedures for $\boldsymbol{\Theta}_1$ and $\boldsymbol{\Theta}_2$. However, it is essential to acknowledge that alternative algorithms can be equally effective in resolving $\boldsymbol{\Theta}_1$ and $\boldsymbol{\Theta}_2$. As previously outlined, the fundamental approach involves the independent decomposition of the two segmented channels within the RIS cascaded channel through SVD, leading to the determination of the two virtual sub-process regulation matrices, $\boldsymbol{\Theta}_1$ and $\boldsymbol{\Theta}_2$, pertinent to the RIS. Subsequently, the comprehensive RIS regulation matrix is computed in accordance with Eq. (10).

The SVD decomposition of two segmented channels $\boldsymbol{G}_{\mathrm{NB-RIS}}$ and $\boldsymbol{H}_{\mathrm{RIS-UE}}^{\mathrm{H}}$ can be expressed as Eq. (12).

$$\begin{cases} \mathrm{SVD}(\boldsymbol{G}_{\mathrm{NB-RIS}}) = \boldsymbol{U}_G \boldsymbol{D}_G \boldsymbol{V}_G^{\mathrm{H}}, \\ \mathrm{SVD}(H_{\mathrm{RIS-UE}}^{\mathrm{H}}) = \boldsymbol{U}_H \boldsymbol{D}_H \boldsymbol{V}_H^{\mathrm{H}} \end{cases} \tag{12}$$

The receiving matrix of segmented channel $\boldsymbol{G}_{\mathrm{NB-RIS}}$ is $\boldsymbol{V}_G$, and that of segmented channel $\boldsymbol{H}_{\mathrm{RIS-UE}}^{\mathrm{H}}$ is $\boldsymbol{U}_H^{\mathrm{H}}$.

Compared with Eq. (10), if $\boldsymbol{\Theta}_1 = \boldsymbol{U}_G^{\mathrm{H}}$ and $\boldsymbol{\Theta}_2 = \boldsymbol{V}_H$ are given, Eq. (10) can be transformed into Eq. (13).

$$\boldsymbol{\Theta} = \boldsymbol{\Theta}_2 \boldsymbol{\Theta}_1 = \boldsymbol{V}_H \boldsymbol{U}_G^{\mathrm{H}} \tag{13}$$

If Eq. (13) is introduced into Eq. (11), it will be updated and represented as Eq. (14).

$$\boldsymbol{H}_{\mathrm{DL}} = \boldsymbol{H}_{\mathrm{RIS-UE}}^{\mathrm{H}} \Theta_2 \boldsymbol{\Theta}_1 \boldsymbol{G}_{\mathrm{NB-RIS}} = (\boldsymbol{H}_{\mathrm{RIS-UE}}^{\mathrm{H}} \boldsymbol{V}_H \boldsymbol{U}_G^{\mathrm{H}} \boldsymbol{G}_{\mathrm{NB-RIS}}) \tag{14}$$

By combining Eq. (14) with Eq. (9), the received signal $\boldsymbol{Y}_{\mathrm{DL,UE}}$ at the UE side can be expressed as Eq. (15).

$$\boldsymbol{Y}_{\mathrm{DL,UE}} = \boldsymbol{H}_{\mathrm{RIS-UE}}^{\mathrm{H}} \boldsymbol{V}_H \boldsymbol{U}_G^{\mathrm{H}} \boldsymbol{G}_{\mathrm{NB-RIS}} \boldsymbol{F}\boldsymbol{x} + \boldsymbol{W} \tag{15}$$

In addition, SVD is a unitary transformation operation of the matrix, which meets the constant modulus criterion of the RIS regulation matrix. That is, if $\boldsymbol{\Theta}_1 = \boldsymbol{U}_G^{\mathrm{H}}$ is a unitary matrix and $\boldsymbol{\Theta}_2 = \boldsymbol{V}_H$ is a unitary matrix, then $\boldsymbol{\Theta} = \boldsymbol{V}_H \boldsymbol{U}_G^{\mathrm{H}}$ is also a unitary matrix.

The achievable rate R of a RIS-assisted MIMO system is given in Eq. (16).

$$R = B\log_2 \det\left(\boldsymbol{I}_K + \frac{\rho}{N\sigma^2} \boldsymbol{H}_{\mathrm{DL}} \boldsymbol{F}\boldsymbol{F}^{\mathrm{H}} \boldsymbol{H}_{\mathrm{DL}}^{\mathrm{H}}\right) \tag{16}$$

According to the previous discussion, the relevant variable expressions of Eq. (10) are substituted. Then, Eq. (16) can be expressed as Eq. (17).

$$R = B\log_2 \det\Bigg(\boldsymbol{I}_K + \frac{\rho}{N\sigma^2} (\boldsymbol{H}_{\mathrm{RIS-UE}}^{\mathrm{H}} \boldsymbol{V}_H \boldsymbol{U}_G^{\mathrm{H}} \boldsymbol{G}_{\mathrm{NB-RIS}}) \cdot \boldsymbol{F}\boldsymbol{F}^{\mathrm{H}} (\boldsymbol{H}_{\mathrm{RIS-UE}}^{\mathrm{H}} \boldsymbol{V}_H \boldsymbol{U}_G^{\mathrm{H}} \boldsymbol{G}_{\mathrm{NB-RIS}})^{\mathrm{H}}\Bigg) \tag{17}$$

where B is the occupied frequency bandwidth, ρ is the transmission power of the NB, and σ is the variance of Gaussian white noise corresponding to $\boldsymbol{W}$.

An alternative strategy involves the utilization of conventional classical optimization techniques to determine the regulation matrix components $\boldsymbol{\Theta}_1$ and $\boldsymbol{\Theta}_2$ for the two virtual regulation sub-processes, respectively. Extensive discourse on relevant optimization algorithms can be found in existing literature. This article focuses on presenting the optimization problem and its associated constraints, as exemplified in Formula (18). Elaborations on specific solutions will not be reiterated here.

$$\begin{aligned} \max_{\forall \vartheta_i} \ & R_{\mathrm{sum}} = \sum_{k=1}^{K} f(\boldsymbol{G}_k, \boldsymbol{H}_k, \boldsymbol{F}_k, p_k) \\ \text{s.t.} \ & \|\theta_i\| = 1, \forall \theta_i; \\ & \sum_{k=1}^{K} p_k \leqslant p; \\ & \|\boldsymbol{F}_k\| = 1, k = 1, 2, \ldots, K \end{aligned} \tag{18}$$

where $\boldsymbol{G}_k$, $\boldsymbol{H}_k^{\mathrm{H}}$, and $\boldsymbol{F}_k$ are the channel components of $\boldsymbol{u}_k$ and the multi-antenna precoding matrix on the NB side for the $\boldsymbol{u}_k'$'s signal, respectively; θ_i is the regulation coefficient of the i-th element of RIS; p_k is the allocated power for $\boldsymbol{u}_k$, satisfying $\sum_{k=1}^{K} p_k \leqslant p_{\max}$; K is the total number of UE, and $p_{\max}$ is the maximum rated transmission power of the base station.

Get $\boldsymbol{\Theta}_1 = \vartheta_{1,\mathrm{opt}}$ and $\boldsymbol{\Theta}_2 = \vartheta_{2,\mathrm{opt}}$ respectively, and then get expression (19) according to Eq. (10).

$$\boldsymbol{\Theta} = \boldsymbol{\Theta}_2 \boldsymbol{\Theta}_1 = \vartheta_{2,\mathrm{opt}} \vartheta_{1,\mathrm{opt}} \tag{19}$$

3.3 Channel decoupling multi-user access

In the context of multi-user access scenarios, while preserving generality, this article will explore multi-user access utilizing orthogonal frequency division multiple access (OFDMA) and will consider two user equipments (UEs), denoted as UE_1 and UE_2, for illustrative purposes. Due to the inherent frequency domain orthogonality, it is reasonable to assume the independence of the channels associated with the two UEs, specifically $\boldsymbol{G}_{\mathrm{UE}_1}$ and $\boldsymbol{G}_{\mathrm{UE}_2}$, as well as the independence of $\boldsymbol{H}_{\mathrm{UE}_1}$ and $\boldsymbol{H}_{\mathrm{UE}_2}$.

A pattern addition (PA)-based multi-beam mechanism, as detailed in Ref. [21], can be employed to address the multi-user RIS regulation matrix. That is, the regulation matrices $\boldsymbol{\Theta}_{\mathrm{UE}_1}$ and $\boldsymbol{\Theta}_{\mathrm{UE}_2}$ of UE_1 and UE_2 are solved respectively, and then the complete regulation matrix of RIS for two UEs is obtained using the PA mechanism. Without loss of generality, SVD remains the chosen method for resolving the regulation matrices of UE_1 and UE_2.

The expressions to solve the regulation matrix corresponding to UE_1 are given by Eqs. (20) and (21).

$$\begin{cases} \mathrm{SVD}(\boldsymbol{G}_{\mathrm{UE}_1}) = \boldsymbol{U}_{G,\mathrm{UE}_1} \boldsymbol{D}_{G,\mathrm{UE}_1} \boldsymbol{V}_{G,\mathrm{UE}_1}^{\mathrm{H}}, \\ \mathrm{SVD}(\boldsymbol{H}_{\mathrm{UE}_1}^{\mathrm{H}}) = \boldsymbol{U}_{H,\mathrm{UE}_1} \boldsymbol{D}_{H,\mathrm{UE}_1} \boldsymbol{V}_{H,\mathrm{UE}_1}^{\mathrm{H}} \end{cases} \tag{20}$$

$$\boldsymbol{\Theta}_{\mathrm{UE}_1} = \boldsymbol{\Theta}_{\mathrm{UE}_1,2} \boldsymbol{\Theta}_{\mathrm{UE}_1,1} = \boldsymbol{V}_{H,\mathrm{UE}_1} \boldsymbol{U}_{G,\mathrm{UE}_1}^{\mathrm{H}} \tag{21}$$

The expressions for solving the corresponding regulation matrix of UE_2 are Eqs. (22) and (23).

$$\begin{cases} \mathrm{SVD}(\boldsymbol{G}_{\mathrm{UE}_2}) = \boldsymbol{U}_{G,\mathrm{UE}_2} \boldsymbol{D}_{G,\mathrm{UE}_2} \boldsymbol{V}_{G,\mathrm{UE}_2}^{\mathrm{H}}, \\ \mathrm{SVD}(\boldsymbol{H}_{\mathrm{UE}_2}^{\mathrm{H}}) = \boldsymbol{U}_{H,\mathrm{UE}_2} \boldsymbol{D}_{H,\mathrm{UE}_2} \boldsymbol{V}_{H,\mathrm{UE}_2}^{\mathrm{H}} \end{cases} \tag{22}$$

$$\boldsymbol{\Theta}_{\mathrm{UE}_2} = \boldsymbol{\Theta}_{\mathrm{UE}_2,2}\boldsymbol{\Theta}_{\mathrm{UE}_2,1} = \boldsymbol{V}_{H,\mathrm{UE}_2}\boldsymbol{U}^{\mathrm{H}}_{G,\mathrm{UE}_2} \tag{23}$$

Equation (24) based on the PA mechanism is used for two UE, UE_1 and UE_2. The complete regulation matrix $\boldsymbol{\Theta}_{\mathrm{mu}}$ of RIS is obtained in Eq. (24).

$$\boldsymbol{\Theta}_{\mathrm{mu}} = \sum_{k=1}^{K}\alpha_k\boldsymbol{\Theta}_k \tag{24}$$

where $\boldsymbol{\Theta}_k$ represents the RIS regulation matrix corresponding to the single connection of UE_k, the complex number $\alpha_k = \rho_k \exp(-\mathrm{j}\vartheta_k)$ represents the weighting coefficient of the regulation matrix component of UE_k satisfying constraint $\sum_{k=1}^{K}\|\alpha_k\|_2 \leqslant 1$, and K represents the total number of UE connected simultaneously.

For $K = 2$, Eqs. (21) and (23) are introduced into Eq. (24), and the final expression of the RIS regulation matrix of UE_1 and UE_2 is obtained (Eq. (25)).

$$\boldsymbol{\Theta}_{mu} = \alpha_{\mathrm{UE}_1}\boldsymbol{\Theta}_{\mathrm{UE}_1} + \alpha_{\mathrm{UE}_2}\boldsymbol{\Theta}_{\mathrm{UE}_2} \tag{25}$$

4 Numerical simulation

In the preceding sections, we have undertaken an extensive theoretical analysis of the channel decoupling scheme. Building upon these analytical foundations, this section employs the Monte Carlo method to conduct a numerical assessment of the proposed methodology within both single-user and multi-user access scenarios.

4.1 Performance evaluation of single-user cases

In this simulation, we assume a far-field channel model and employ a uniform planar array (UPA) with $M = M_x \times M_y$ elements for the RIS, while fixing $M_x = 50$ and increasing $M_y \in [2,4,8,16,32]$. The base station (BS) uses a UPA with $N = N_x \times N_y$ elements, $N_x = 8$ and $N_y = 4$. The carrier frequency is set to $f_c = 28$ GHz.

We conduct a comparative analysis between the proposed cascaded channel decoupling algorithm (referred to as Eq. (17)) and two established benchmarks: the conventional alternating optimization (AO) algorithm and a baseline method involving random phase regulation. The latter simulates the impact of random scattering on natural surfaces when the RIS is absent.

Figure 2 depicts the achievable data rate versus the number M of RIS elements, where the transmission power p is fixed and M varies. The “Random” curve indicates the performance achieved when the incident electromagnetic wave is randomly scattered; the “Decoupling” curve indicates the performance achieved when the proposed decoupling schemes are used. Analysis of the simulation curves reveals that the proposed algorithm attains performance on par with the traditional AO algorithm, and both exhibit substantial RIS beamforming gains when contrasted with the random phase baseline. These simulation findings affirm the efficacy of the proposed RIS cascaded channel decoupling mechanism as a viable and low-complexity approach for resolving the RIS regulation matrix.

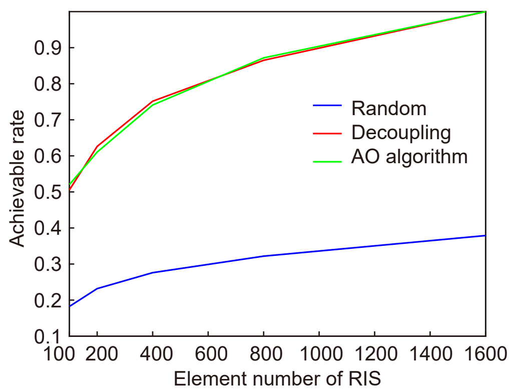

Fig. 2 Performance of single-user cases (note: this figure shows the normalized data rates).

4.2 Performance evaluation of multi-user cases

Assuming two UEs are utilizing OFDMA multiple access and PA mechanism for multi-beam, while using a far-field model channel. The base station's antenna type is ULA, with $M = 64$ antennas, and the RIS antenna type is ULA with $N \in \{800, 1600, 3200, 6400\}$ antenna elements. Additionally, the central frequency is $f_c = 5$ GHz, and the number of users is $K = 2$.

When assessing the performance of multi-UE access utilizing the PA-based approach through the application of Eq. (23), three distinct performance scenarios are presented for comparative analysis: perfect regulation, unexpected regulation, and straightforward signal mirroring. As depicted in the numerical simulation curve within Fig. 3, it is evident that while the PA mechanism does introduce a slight performance diminishment in comparison to the ideal scenario, it nonetheless delivers superior performance gains when juxtaposed with unexpected regulation and straightforward signal mirroring.

The numerical simulation results presented above affirm the effectiveness of the proposed RIS cascaded channel decoupling mechanism as a low-complexity approach for resolving the RIS regulation matrix.

5 Conclusion

In this paper, we introduce a novel decoupling model for the RIS cascaded channel, which breaks down the electromagnetic wave regulation process performed by the RIS into two distinct sub-processes: the virtual receiving response and virtual regulation transmission. This division results in the dissection of the RIS regulation matrix into two key constituents: the receiving response matrix and the regulation transmission matrix. Leveraging this cascaded channel decoupling mechanism, we can independently solve two segmented channels, considerably streamlining the computation of the RIS regulation matrix. The article further delves into the proposed decoupling methodology, examining its applicability in two scenarios: single-UE access and multi-UE access, and presenting corresponding solutions. Our numerical simulation results conclusively demonstrate that the suggested channel decoupling scheme represents a low-complexity and highly effective approach for resolving the RIS regulation matrix.

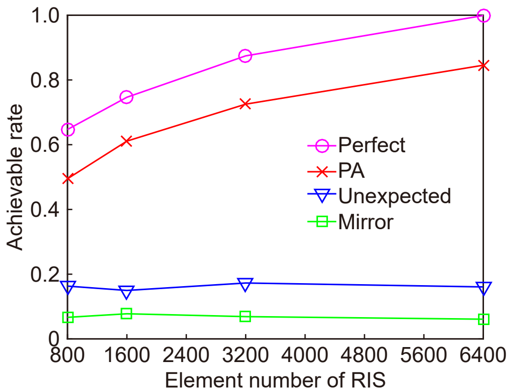

Fig. 3 Performance of multi-user cases "perfect" means the best performance without considering the constraints specified by RIS and represents the upper bound of performance. "PA" indicates the use of PA mechanism. "Unexpected" indicates that the signal is subject to unexpected abnormal regulation. "Mirror" indicates simple mirror regulation of the signal.

Future research endeavors should focus on the detailed implementation and comprehensive performance assessment of various sub-regulation matrix techniques for resolving segmented channels. Furthermore, there is a pressing need for further investigation into the specific implementation and performance evaluation of RIS channel models capable of concurrently including cascading and direct channel components. These avenues of research hold the potential to advance the understanding and applicability of RIS technology in wireless communication systems.

References

[1] Y. Yuan, Y. Zhao, B. Zong, and S. Parolari, Potential key technologies for 6G mobile communications, *Sci. China Inf. Sci.*, vol. 63, no. 8, p. 183301, 2020.

[2] IMT-2030 (6G) Promotion Group, Research report on reconfigurable intelligent surface (RIS), https://www.imt2030.org.cn/html/default/zhongwen/chengguofabu/yanjiubaogao/index.html?index=2, 2021.

[3] M. Di Renzo, A. Zappone, M. Debbah, M. S. Alouini, C. Yuen, J. de Rosny, and S. Tretyakov, Smart radio environments empowered by reconfigurable intelligent surfaces: How it works, state of research, and the road ahead, *IEEE J. Select. Areas Commun.*, vol. 38, no. 11, pp. 2450–2525, 2020.

[4] H. Jiang, B. Xiong, H. Zhang, and E. Başar, Physics-based 3D end-to-end modeling for double-RIS assisted non-stationary UAV-to-ground communication channels, *IEEE Trans. Commun.*, vol. 71, no. 7, pp. 4247–4261, 2023.

[5] H. Jiang, B. Xiong, H. Zhang, and E. Basar, Hybrid far- and near-field modeling for reconfigurable intelligent surface assisted V2V channels: A sub-array partition based approach, *IEEE Trans. Wireless Commun.*, vol. 22, no. 11, pp. 8290–8303, 2023.

[6] C. Huang, Z. Yang, G. C. Alexandropoulos, K. Xiong, L. Wei, C. Yuen, Z. Zhang, and M. Debbah, Multi-hop RIS-empowered terahertz communications: A DRL-based hybrid beamforming design, *IEEE J. Select. Areas Commun.*, vol. 39, no. 6, pp. 1663–1677, 2021.

[7] X. Guan, Q. Wu, and R. Zhang, Joint power control and

passive beamforming in IRS-assisted spectrum sharing, *IEEE Commun. Lett.*, vol. 24, no. 7, pp. 1553–1557, 2020.

[8] M. Hua and Q. Wu, Joint dynamic passive beamforming and resource allocation for IRS-aided full-duplex WPCN, *IEEE Trans. Wirel. Commun.*, vol. 21, no. 7, pp. 4829–4843, 2022.

[9] Q. Wu, X. Zhou, W. Chen, J. Li, and X. Zhang, IRS-aided WPCNs: A new optimization framework for dynamic IRS beamforming, *IEEE Trans. Wirel. Commun.*, vol. 21, no. 7, pp. 4725–4739, 2022.

[10] Z. Li, W. Chen, and H. Cao, Beamforming design and power allocation for transmissive RMS-based transmitter architectures, *IEEE Wirel. Commun. Lett.*, vol. 11, no. 1, pp. 53–57, 2022.

[11] Y. Zhao and X. Lv, Network coexistence analysis of RIS-assisted wireless communications, *IEEE Access*, vol. 10, pp. 63442–63454, 2022.

[12] Y. Zhao and M. Jian, Applications and challenges of Reconfigurable Intelligent Surface for 6G networks, arXiv preprint arXiv: 2108.13164, 2021.

[13] Y. Zhao. Reconfigurable intelligent surfaces for 6G: applications, challenges and solutions. *Frontiers of Information Technology & Electronic Engineering*, 2023.

[14] P. Wang, J. Fang, L. Dai, and H. Li, Joint transceiver and large intelligent surface design for massive MIMO mmWave systems, *IEEE Trans. Wirel. Commun.*, vol. 20, no. 2, pp. 1052–1064, 2021.

[15] S. Abeywickrama, R. Zhang, Q. Wu, and C. Yuen, Intelligent reflecting surface: Practical phase shift model and beamforming optimization, *IEEE Trans. Commun.*, vol. 68, no. 9, pp. 5849–5863, 2020.

[16] X. Li, X. Wang, X. Hou, L. Chen, and S. Suyama, Two-step beamforming scheme for large-dimension reconfigurable intelligent surface, in *Proc. IEEE 95th Vehicular Technology Conference*, Helsinki, Finland, 2022, pp. 1–5.

[17] B. Ning, Z. Chen, W. Chen, and J. Fang, Beamforming optimization for intelligent reflecting surface assisted MIMO: A sum-path-gain maximization approach, *IEEE Wirel. Commun. Lett.* , p. 1, 2020.

[18] S. Zhang and R. Zhang, Capacity characterization for intelligent reflecting surface aided MIMO communication, *IEEE J. Select. Areas Commun.*, vol. 38, no. 8, pp. 1823–1838, 2020.

[19] X. Wei, D. Shen, and L. Dai, Channel estimation for RIS assisted wireless communications—Part II: An improved solution based on double-structured sparsity, *IEEE Commun. Lett.*, vol. 25, no. 5, pp. 1403–1407, 2021.

[20] G. Zhu, K. Huang, N. Lau V. K. , and B. Xia, X. Li, S. Zhang, Hybrid beamforming via the kronecker decomposition for the millimeter-wave massive MIMO systems, *IEEE J. Sel. Areas Commun*, vol. 35, no. 9, pp. 2097–2114, 2017.

[21] N. M. Tran, M. M. Amri, J. H. Park, D. I. Kim, and K. W. Choi, Multifocus techniques for reconfigurable intelligent surface-aided wireless power transfer: Theory to experiment, *IEEE Internet Things J.*, vol. 9, no. 18, pp. 17157–17171, 2022.

Yajun Zhao holds bachelor, master, and doctoral degrees. Since 2010, he has assumed the role of Chief Engineer within the Wireless and Computing Product R&D Institute at ZTE Corp. Prior to this, he contributed to wireless technology research within the Wireless Research Department at Huawei. Currently, his primary focus centers on 5G standardization technology and the advancement of future mobile communication technology, particularly 6G. His research pursuits encompass a broad spectrum, including reconfigurable intelligent surfaces (RIS), spectrum sharing, flexible duplex, CoMP, and interference mitigation. He has played an instrumental role in founding the RIS Tech Alliance (RISTA) and currently holds the position of Deputy Secretary General within the organization. Additionally, he is a founding member of the RIS task group under the purview of the China IMT-2030 (6G) Promotion Group, where he serves as the Deputy Leader.